

Energetics and kinetics of native point defects in Ga₂Se₃ from first principlesGui-Yang Huang^{1,*} and B. D. Wirth^{1,2,†}¹*Department of Nuclear Engineering, University of Tennessee, Knoxville, Tennessee, USA*²*Oak Ridge National Laboratory, Knoxville, Tennessee, USA*

(Received 7 May 2013; revised manuscript received 13 June 2013; published 9 August 2013)

Based on first-principles calculations, the Ga vacancy and antisite defect Se_{Ga} are the only intrinsic shallow acceptors in Ga₂Se₃. The Ga interstitial is always a donor, +3 charge state under *p*-type conditions or +1 charge state under *n*-type conditions. Both the Se vacancy and Se interstitial are neutral defects except under an extremely *p*-type condition. Both the Ga interstitial and Se interstitial are predicted to be a very fast diffuser under *n*-type conditions, with a migration barrier value of <0.3 eV. Under *p*-type conditions, the calculated migration barrier of the Ga interstitial has a quite large value of >1.0 eV. The +2 charge state is stable for the Se interstitial under the extremely *p*-type condition, and the corresponding migration barrier is 0.68 eV. The migration barriers of the Ga vacancy and Se vacancy are >0.8 eV and >1.3 eV, respectively.

DOI: [10.1103/PhysRevB.88.085203](https://doi.org/10.1103/PhysRevB.88.085203)

PACS number(s): 61.72.jd, 61.66.Dk, 66.30.Fq, 31.15.A—

I. INTRODUCTION

Ga₂Se₃ is a III-VI compound semiconductor, with a defect zinc blende structure in which 1/3 cation sites are vacant. This class of material is potentially applicable for nuclear particle detection or semiconductor devices operating in high radiation environments, due to its anomalously high radiation stability,^{1–3} which may originate from a large number of structural vacancies and the small migration barriers of interstitial atoms. For room temperature radiation detector applications, an appropriate band gap (>1.4 eV) is required. The reported band gaps for Ga₂Te₃ and Ga₂Se₃ are 1.0–1.2 eV^{4–10} and 2.0–2.6 eV,^{11,12} respectively. Complete solid solutions of Ga₂Se₃ and Ga₂Te₃ throughout the whole range of composition can be achieved,^{13,14} although solid-state immiscibility is also reported to exist between $x = 0.50$ and $x = 0.90$ for Ga₂(Se_{*x*}Te_{1–*x*})₃ under certain conditions.¹⁵ Therefore the ternary Ga₂(Se_{*x*}Te_{1–*x*})₃ system was recently proposed to obtain an appropriate band gap for the room temperature radiation detector applications.¹⁶ Previously, a large single crystal of Ga₂Te₃ and Ga₂(Se_{*x*}Te_{1–*x*})₃ was successfully grown by the Bridgman method,¹⁶ while we investigated the structure and band structure of vacancy-ordered Ga₂Se₃.¹⁷ In this paper, we describe the energetics and kinetics of the native point defects in Ga₂Se₃. As known, the carrier concentration, carrier mobility, carrier lifetime, creation energy of Frenkel pairs, and migration energy of intrinsic point defects are essential properties to understand and design nuclear radiation detectors. The carrier concentration depends on the concentration and charge transition level of intrinsic point defects. The carrier lifetime depends on the concentration of deep-level intrinsic point defects. The carrier mobility depends on the crystal quality (concentration of point defects, migration energy of point defects, etc.). The doping may be investigated in the future; however it is not included here. The results of Ga₂Te₃ and Ga₂(Se_{*x*}Te_{1–*x*})₃ will be reported in the near future, together with the experimental measurements of the band gap. At present, relevant theory investigations are very deficient for Ga₂Se₃.

Vacancy-ordered bulk and epitaxial thin films Ga₂Se₃ can be grown with a slight excess of Se and with a high Se/Ga ratio above 150, respectively. It is possible that a high concentration

of extra Ga vacancy, Se interstitial, or Se_{Ga} antisite defects exists in the sample. However, as-grown Ga₂Se₃ crystals often have a high resistivity and low carrier concentration.^{18,19} The high resistivity can be attributed to the low concentration of intrinsic point defects, or the ionization energy of intrinsic point defects is high, or there exists high self-compensation of donor and acceptor defects. Although the deep-level defects do not contribute to the carrier concentration, they can influence the carrier lifetime. Therefore, they should also be included and investigated.

In the literature, both *p*-type^{20–23} and *n*-type¹⁹ conductivities have been reported for the undoped Ga₂Se₃. Whether the conductivities should be attributed to the native point defects is unclear. Formation energy and defect (charge) transition level calculations can clarify these problems.

High radiation stability has been reported for the III-VI compound semiconductors.^{1–3} The fast diffusion of interstitial atoms due to the existence of a large amount of structural vacancies may be responsible for the anomalously high radiation stability. The comprehensive investigation of the diffusion behavior of native point defects is useful for understanding these problems.

Although first-principles calculations have been used extensively to investigate the formation energy, defect transition levels, and diffusion behavior of point defects in other semiconductors (for example, ZnO), no work on point defects of Ga₂Se₃ has been reported to date. Here, we describe a comprehensive investigation for Ga₂Se₃, which should also be useful for other III-VI compound semiconductors.

II. CALCULATIONAL METHOD AND MODELS

The density functional calculations were performed using the plane-wave-based Vienna Ab initio Simulation Package (VASP),^{24,25} based on the local density approximation (LDA)²⁶ and generalized-gradient approximation (GGA-PBE).²⁷ The electron wave functions were described using the projector augmented wave (PAW) method of Blöchl²⁸ in the implementation of Kresse and Joubert.²⁹ Plane waves have been included up to a cutoff energy of 211.534 eV. Electronic states were occupied with a Gaussian smearing width of 0.1 eV. A real-space projection scheme was used for efficient

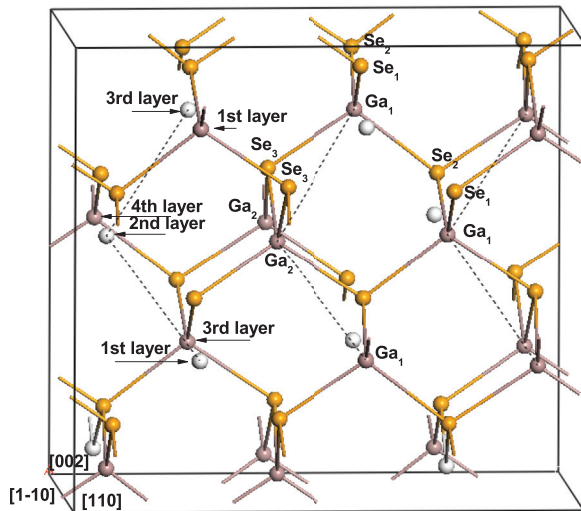


FIG. 1. (Color online) Structure of mono-Ga₂Se₃. The white balls denote vacancies.

computations of supercells with >20 atoms. Wave function optimization was truncated when the energy difference was less than 1×10^{-5} eV. The optimization procedure was truncated when the residual forces for the relaxed atoms were less than 0.01 eV/Å. For supercell calculations, the shape and volume of the supercell are fixed to the theoretical value of perfect supercell.

Monoclinic and orthorhombic Ga₂Se₃ are denoted by mono- and ortho-Ga₂Se₃, respectively. The supercell is based on the orthorhombic unit cell. For mono-Ga₂Se₃, the building unit cell is shown in Fig. 1 (40 atoms). The lattice parameters are $a_1 = 12.01$ Å, $a_2 = 7.94$ Å, and $a_3 = 11.03$ Å (PBE). A $2 \times 3 \times 2$ supercell denotes a supercell with $2a_1$, $3a_2$, and $2a_3$ lattice parameters. $2 \times 3 \times 2$ is also denoted by 232 in the tables. In a PBE calculation, the unit cell is not rigorously orthorhombic, whereas in a LDA calculation, the unit cell is orthorhombic. For ortho-Ga₂Se₃, the building unit cell is quite simple and not shown here (10 atoms). Its structure has been shown in Refs. 30–34. The lattice parameters are $a_1 = 11.83$ Å, $a_2 = 3.91$ Å, and $a_3 = 5.72$ Å (PBE). A $2 \times 6 \times 4$ supercell denotes a supercell with $2a_1$, $6a_2$, and $4a_3$ lattice parameters.

For the hybrid DFT supercell calculations, wave function optimization was truncated when the energy difference was less than 1×10^{-4} eV. The optimization procedure was truncated when the residual forces for the relaxed atoms were less than 0.01 eV/Å. The screened hybrid exchange functional of Heyd, Scuseria, and Ernzerhof (HSE03/HSE06)^{35–37} is adopted here, which should converge more rapidly with respect to the number of k points than PBE0. Therein, HSE03 and HSE06 have a different range separation parameter (HFSCREEN) in range-separated hybrid functionals, corresponding to HFSCREEN=0.3 and HFSCREEN=0.2, respectively. One Γ k point is used. The cell shape and volume are optimized based on the hybrid DFT calculation. Because the GW calculations (very slow) were performed in parallel to the hybrid DFT calculations, and the experimental reported band gap for Ga₂Se₃ is highly uncertain, the default mixing ratio of nonlocal exchange of 0.25 has been used. Tuning the

mixing ratio to reproduce the GW band gap or experimental band gap has not been performed.

In order to obtain the energy barriers for the various diffusion paths, we used the climbing image nudged elastic band method (CI-NEB)^{38,39} as implemented in VASP by Henkelman, Jonsson, and others.⁴⁰ This approach is expected to be more reliable than dragging an atom from minimum to minimum across the estimated or guessed saddle, especially in multiatom migration events. The images of the CI-NEB were relaxed until the maximum residual force was less than 0.01 eV/Å.

For the CI-NEB calculations, one Γ k point has been used. $2 \times 3 \times 2$ and $2 \times 6 \times 4$ supercells are used for mono- and ortho-Ga₂Se₃, respectively. For semiconductors, in general, the CI-NEB calculations need more middle images than metal.^{41,42} Insufficient middle images can induce large error on the migration barrier.^{41,42} The intermediate metastable structures should be identified. The presence of metastable structures between the initial and final configuration is avoided by dividing into several CI-NEB calculations. In this way, it is easier to obtain the convergence. Three or four images are generally used. Because many possible diffusion paths exist, more images are not adopted. This may induce some error. For some diffusion paths, the calculated migration barrier difference between one and three images is large (up to 0.3 eV). However, three or four images should be more or less sufficient for the CI-NEB calculations.

III. FORMATION ENERGY AND TRANSITION LEVELS

A. Theory

The concentration of a point defect depends on its formation energy via $c = N_{\text{sites}} \exp(-E_f/kT)$ under thermodynamic equilibrium conditions^{43–46} (dilute limit approximation). N_{sites} is the lattice point density, E_f is the formation energy of the point defect, k is the Boltzmann constant, and T is the absolute temperature. The formation energy and (charge) transition level of the point defects in semiconductors are well known in the literature, which has been described clearly by Van de Walle.⁴⁵ The definitions of formation energy and transition level are not repeated here. However, it is necessary to discuss several important issues of the first-principles defect calculation. Recently, several review papers about the method of defect calculation have been published, which are provided in Ref. 47 and the references therein.

1. Problem of potential alignment

First, for charged defects, a jellium background charge is added to neutralize the supercell in the calculations. It is believed that for the charged supercell, the supercell energy is no longer well defined and arbitrarily shifted,⁴⁴ or there exist background effects due to the periodic images of the charged defect.⁴⁶ The so-called potential-alignment technique is commonly used to overcome this problem in the literature, in which the electrostatic potential at a position far away from the defect is taken as reference (denoted as reference potential) to adjust the valence band maximum (VBM) of the perfect supercell to obtain the VBM of the charged supercell. However, this potential-alignment technique may suffer from

some problems. For a sufficiently large supercell, the influence of defect rather than the jellium background charge would dominate the shift of the reference potential. At the same time, even for a very large supercell, the reference potential may be severely affected by the defect, as shown in Fig. 1 of Ref. 48. On the other hand, the reference potential is almost insensitive to the charge state of the defect for a sufficiently large supercell according to direct calculation results (if the structure of the point defect with two different charge states does not change significantly), because the influence of point defect for the two different charge state is almost the same. Due to the long-range influence of the defect, the reference potential is very sensitive to the selection of the reference position sometimes (although some authors take the average value at several positions as the reference potential to reduce the sensitivity). Therefore, the commonly used potential-alignment technique may actually suffer from problems. As pointed out by Nieminen,⁴⁶ the potential-alignment technique is inaccurate in cases where the potential varies considerably in the outer regions of the supercell. On the other hand, it is also unnecessary for a sufficiently large supercell, as already shown by Lany *et al.*⁴⁴

In the literature, some authors have tried to eliminate the long-range influence of the defect^{49,50} on the electrostatic potential. In this way, the problem of potential alignment can be resolved. However, we have not chosen to adopt this method due to complexity. When the supercell is sufficiently large, such potential alignment should be very small.^{44,49}

2. VBM alignment

According to our calculations, when using a sufficiently large supercell, the conduction band minimum (CBM) is almost unchanged for the acceptors. This indicates that there is not a shift of the band structure of the neutral and charged supercell (with point defect). So the energy of the charged supercell should be actually well defined and not shifted. For a smaller supercell, the CBM is shifted slightly, and the shift is almost the same for different charge states. Therefore the shift is likely due to the incorporation of the defect, but not the effects of jellium background charge. Nevertheless, based on an extensive direct comparison with the calculated transition levels using a larger supercell, the shift should be included to produce a better converged value for a relatively small supercell. That is to say, the alignment technique using the CBM as an alignment reference can improve the convergence, although the shift is due to the point defect, not the jellium background charge. For the donor-type defect, the VBM can be used as an alignment reference, but it does not produce better results than those without alignment (as will be shown later) in our calculations. The reason may be that the Ga interstitial introduces an extra defect level in the band gap, which will affect the VBM. That is to say, both the VBM and CBM are influenced to some extent. As shown later, the VBM alignment is not very important; both the aligned and unaligned results seem to converge to the same result. Therefore although VBM alignment is included in some cases and is not included in some other cases, this introduces only a small uncertainty and difference due to the use of a large supercell.

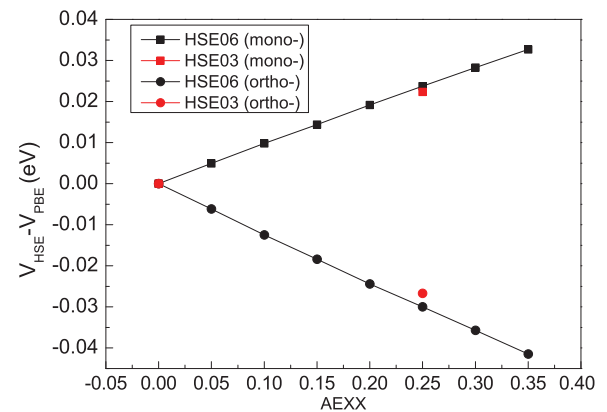


FIG. 2. (Color online) Electrostatic potential shift as a function of mixing ratio (AEXX) of HSE.

3. Average electrostatic potential among different calculation methods

Alkauskas *et al.*^{51–53} observed an important phenomenon that when the electrostatic potentials of different methods are aligned, the transition levels of deep-level defects are close to each other, which has been confirmed by Komsa *et al.*⁵⁵ and Ramprasad *et al.*⁵⁶ Therefore, the electrostatic potential may play an important role as a common reference for different calculation methods.

The dependence of the electrostatic potential on the fraction of nonlocal exchange is shown in Fig. 2. This indicates that the influence of mixing ratio on the electrostatic potential is very weak, compared with the large influence of mixing ratio (AEXX) on the VBM and CBM as shown in our previous paper.¹⁷ The potential shift is calculated based on exactly the same structure (optimized by HSE) for both HSE and PBE. Due to the same structure, the potential shift can be determined precisely. However, the optimized structure based on HSE and PBE is slightly different, so a proper definition of the average electrostatic potential is necessary to calculate potential electrostatic shift for two different structures. However, we have not investigated this effect here.

B. Native point defects in mono-Ga₂Se₃

The structures of both mono- and ortho-Ga₂Se₃ have been described previously,¹⁷ and are not repeated here.

1. Native point defect definition

According to Newman,³⁰ an atom on a structural vacancy should be regarded as an interstitial atom. The extra Ga vacancy is different from the structural stoichiometric vacancy. We view an extra Ga vacancy as a Ga vacancy, and a structural vacancy as an interstitial site. The native point defects are denoted by $V_{\text{Ga}1}$, $V_{\text{Ga}2}$, $\text{Se}_{\text{Ga}1}$, $\text{Se}_{\text{Ga}2}$, $V_{\text{Se}1}$, $V_{\text{Se}2}$, $V_{\text{Se}3}$, $\text{Ga}_{\text{Se}1}$, $\text{Ga}_{\text{Se}2}$, $\text{Ga}_{\text{Se}3}$, I_{Ga} , and I_{Se} . A detailed description of the structure can be found in our previous paper.¹⁷ The denotations correspond to those shown in Fig. 1. For example, $V_{\text{Ga}1}$ denotes a vacancy on a Ga₁ site. $\text{Se}_{\text{Ga}1}$ denotes a Se on a Ga₁ site (antisite defect). I_{Ga} denotes an extra Ga on a structural vacancy site, which can be regarded as a Ga interstitial.

TABLE I. Transition level ($0/-1$) of V_{GaI} of mono- Ga_2Se_3 (in eV). The charge transition levels are defined with respect to the VBM.

($0/-1$)	k point	232	332	333	343	353	453	454
Mono	111	0.053	0.065	0.067	0.069	0.077	0.083	0.083
	222	0.041	0.062	0.058	0.067	0.075	0.082	

2. Convergence test of k -point sampling and supercell size

We use V_{GaI} to check the convergence of k -point sampling and supercell size effects (PBE). We focus on the transition level first, but not the formation energy. The results are summarized in Table I. We can see that a $4 \times 5 \times 3$ supercell and $1 \times 1 \times 1$ Γ k point should be sufficient. However, the $4 \times 5 \times 3$ supercell is too large to be adopted due to the large computational cost of hybrid DFT calculations (HSE03/06). Therefore a $2 \times 3 \times 2$ supercell and $1 \times 1 \times 1$ Γ k point have been used for the hybrid DFT calculations (HSE06). We adopted HSE06, because HSE06 produces a larger band gap than HSE03, which is closer to the experimental band-gap value, with the default fraction (0.25) of the exact exchange and PBE exchange.

3. Se-rich condition and Se-poor condition

The formation energy of point defects in Ga_2Se_3 is dependent on the chemical potential of Ga and Se. According to the phase diagram⁵⁷ of the Ga-Se system, the chemical potential of Ga and Se are limited by (equilibrating with) Se and GaSe. When Ga_2Se_3 is equilibrating with Se, it is called a Se-rich condition (or Ga-poor condition). When Ga_2Se_3 is equilibrating with GaSe, it is called a Se-poor condition (or Ga-rich condition). (See the paper of Van de Walle⁴⁵ for some general understanding.) When the Se/Ga ratio becomes larger, it becomes more ‘‘Se-rich.’’ According to Persin *et al.*,⁵⁸ partial decomposition of Ga_2Se_3 into GaSe occurred at higher substrate temperatures for their sample. According to Lubbers *et al.*,⁵⁹ after the annealing of β Ga_2Se_3 , Se in elemental form is still found besides the compound. Therefore, both the Se-rich condition and Se-poor condition seem to be reachable under certain experimental conditions. However, it should be noticed that the Ga_2Se_3 samples of Persin *et al.*⁵⁸ are polycrystalline, and have disordered vacancies as well.

According to Mikkelsen,⁶⁰ the vacancy-ordered bulk sample needs to be grown with a slight excess of Se.⁶⁰ Ga-rich samples will not transform to the β phase (vacancy-ordered phase) under any conditions.⁶⁰ On the other hand, the vacancy-ordered thin film needs to be grown with a high Se/Ga ratio above 150 on appropriate substrates (GaP, GaAs, etc.).^{32,33} This indicates that both the vacancy-ordered bulk sample and thin film need to be grown or annealed under Se-rich conditions. The observation that a nominal stoichiometric amount of Ga and Se is unnecessary for the growth of Ga_2Se_3 thin film may be due to the effective Se/Ga ratio being different from the apparent Se/Ga ratio.

4. The formation enthalpy of mono- Ga_2Se_3 and ϵ -GaSe

Elemental Ga and Se are taken as the initial state to define the formation enthalpy. The calculated formation enthalpy

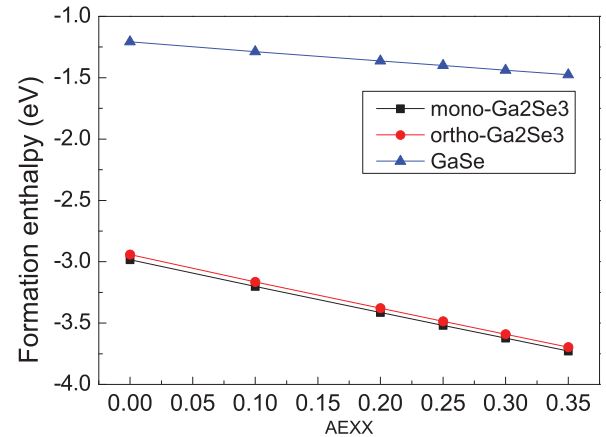


FIG. 3. (Color online) Formation enthalpy as a function of mixing ratio (AEXX).

at 0 K for mono- Ga_2Se_3 is -2.98 eV (per Ga_2Se_3 formula unit) using PBE, -2.79 eV using LDA, and -3.51 eV using HSE06(PBE). Zheng *et al.*⁵⁷ have summarized the experimental formation enthalpy of Ga_2Se_3 at 298 K, from -4.77 to -3.82 eV. According to the thermodynamic model of Zheng *et al.*,⁵⁷ the formation enthalpy at 0 K is -4.39 eV. We can see that HSE06 can improve the calculated formation enthalpy, but there still is a large discrepancy with the experimental value. This indicates that the calculated formation energy of the point defect may have more or less a large error. In addition, although LDA predicts better lattice constants than GGA(PBE),¹⁷ GGA predicts a better formation enthalpy than LDA.

The calculated formation enthalpy of ϵ -GaSe at 0 K is -1.21 eV for PBE, -1.11 eV for LDA, and -1.40 eV for HSE06(PBE). Zheng *et al.*⁵⁷ have summarized the experimental formation enthalpy of GaSe at 298 K, which has values from -1.65 to -1.52 eV. According to the thermodynamic model of Zheng *et al.*,⁵⁷ the formation enthalpy at 0 K is -1.74 eV. The calculation tends to underestimate the formation enthalpy of ϵ -GaSe. Therein, GGA predicts a better formation enthalpy than LDA.

5. The influence of mixing ratio (AEXX) on the calculated formation enthalpy

Calculated formation enthalpy as a function of the mixing ratio (AEXX) is shown in Fig. 3. The formation enthalpy is almost linearly dependent on the mixing ratio. The slope is nearly the same for mono- and ortho- Ga_2Se_3 , but different for GaSe. This indicates that the allowed theoretical range of chemical potential is dependent on the mixing ratio (AEXX), and the relative stability of mono- and ortho- Ga_2Se_3 is independent of the mixing ratio.

6. The chemical potential of Ga and Se

The formation energy of point defects is very sensitive to the chemical potential of Ga and Se. It is necessary to investigate this in more detail and to compare between different calculation methods.

In the literature, the relative chemical potential is often adopted.^{43,61} Relative chemical potential $\Delta\mu_{\text{Ga}}$ and $\Delta\mu_{\text{Se}}$ are defined via $\mu_{\text{Ga}} = \mu_0(\text{Ga}) + \Delta\mu_{\text{Ga}}$ and $\mu_{\text{Se}} = \mu_0(\text{Se}) + \Delta\mu_{\text{Se}}$. Therein $\mu_0(\text{Ga})$ and $\mu_0(\text{Se})$ are the

TABLE II. The chemical potential of Ga and Se (in eV). Δ denotes the difference between Se-rich and Se-poor condition.

		$\Delta\mu_{\text{Ga}}$	$\Delta\mu_{\text{Se}}$	$\Delta\mu_{\text{Ga}} - \Delta\mu_{\text{Se}}$
LDA	Se-rich	-1.40	0	-1.40
	Se-poor	-0.53	-0.58	0.05
	Δ	0.87	-0.58	1.45
PBE	Se-rich	-1.49	0	-1.49
	Se-poor	-0.63	-0.58	-0.05
	Δ	0.86	-0.58	1.44
HSE06(PBE)	Se-rich	-1.76	0	-1.76
	Se-poor	-0.68	-0.72	0.04
	Δ	1.08	-0.72	1.80

chemical potential of the elemental Ga (Ga crystal) and Se (Se crystal).

Based on the free energy minimum principle and the phase diagram,⁵⁷ the theoretical range of chemical potential of Ga and Se can be determined. Temperature, entropy, pressure, and volume effects are neglected. This means that the range of chemical potential may not be very accurate. The results are shown in Table II. We can see that the allowed theoretical range is different for PBE and HSE06 (PBE). The formation enthalpy difference between mono and ortho structure is only 0.038 eV/formula unit,¹⁷ so the chemical potential range of Ga and Se adopts the same value for ortho-Ga₂Se₃ in this paper for simplicity.

7. Spurious effects due to periodic images interaction for the charged point defect

For the neutral point defect, the interaction due to finite supercell size is small. According to our calculations, the formation energy difference using $2 \times 3 \times 2$ and $4 \times 5 \times 4$ supercells for both neutral $V_{\text{Ga}1}$ and I_{Ga} is about 0.01 eV. Oba *et al.*⁶² observed the calculated formation energy of neutral oxygen vacancy in ZnO depends only slightly on cell size, whereas the neutral Zn interstitial shows a strong and nearly linear L^{-1} dependence (the left panel of Fig. 1 in Ref. 62). The slope is almost identical to that for Zn_i^{2+} .⁶² Oba *et al.*⁶² thought the reason is that there are delocalized conduction band electrons (or valence-band holes) constituting the extended defect states, leading to incomplete screening of the defect charge within the supercell. However, such behavior is not consistent with our observations. According to our calculations, I_{Ga} introduces an occupied defect level (two electrons) in the band gap, and the conduction band is occupied by one electron. This is very similar to the Zn interstitial in ZnO (where the conduction band is occupied by two electrons). According to our calculations for $2 \times 3 \times 2$, $3 \times 3 \times 2$, $3 \times 3 \times 3$, $3 \times 4 \times 3$, $3 \times 5 \times 3$, $4 \times 5 \times 3$, and $4 \times 5 \times 4$ supercells, the calculated formation energy difference of the neutral Ga interstitial is less than 0.01 eV, which indicates that the interaction of the neutral Ga interstitial is very small.

For the charged defect, the finite supercell effects are larger. The formation energy as a function of $1/N_{\text{cells}}$ is shown in Fig. 4, where N_{cells} denotes the number of unit cells in the

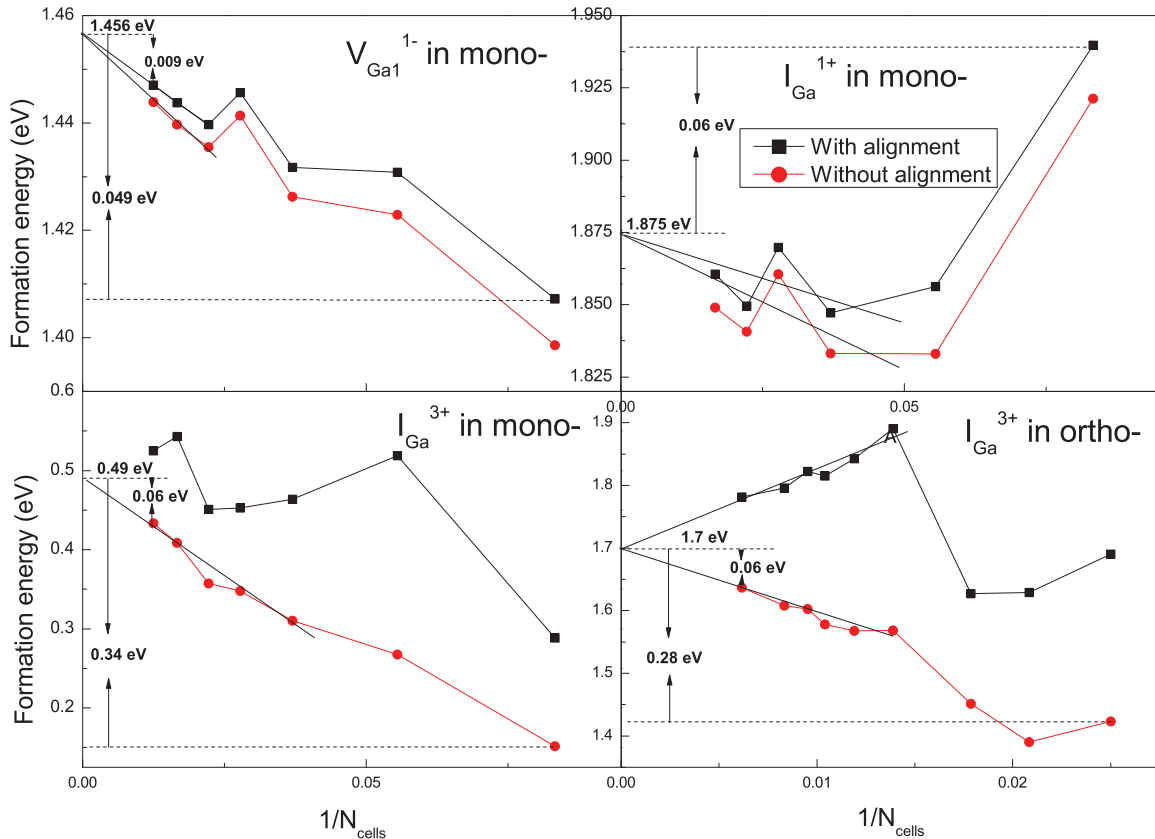


FIG. 4. (Color online) Spurious effects due to periodic images interaction for the charged defect. N_{cells} denotes the number of unit cells in the supercell.

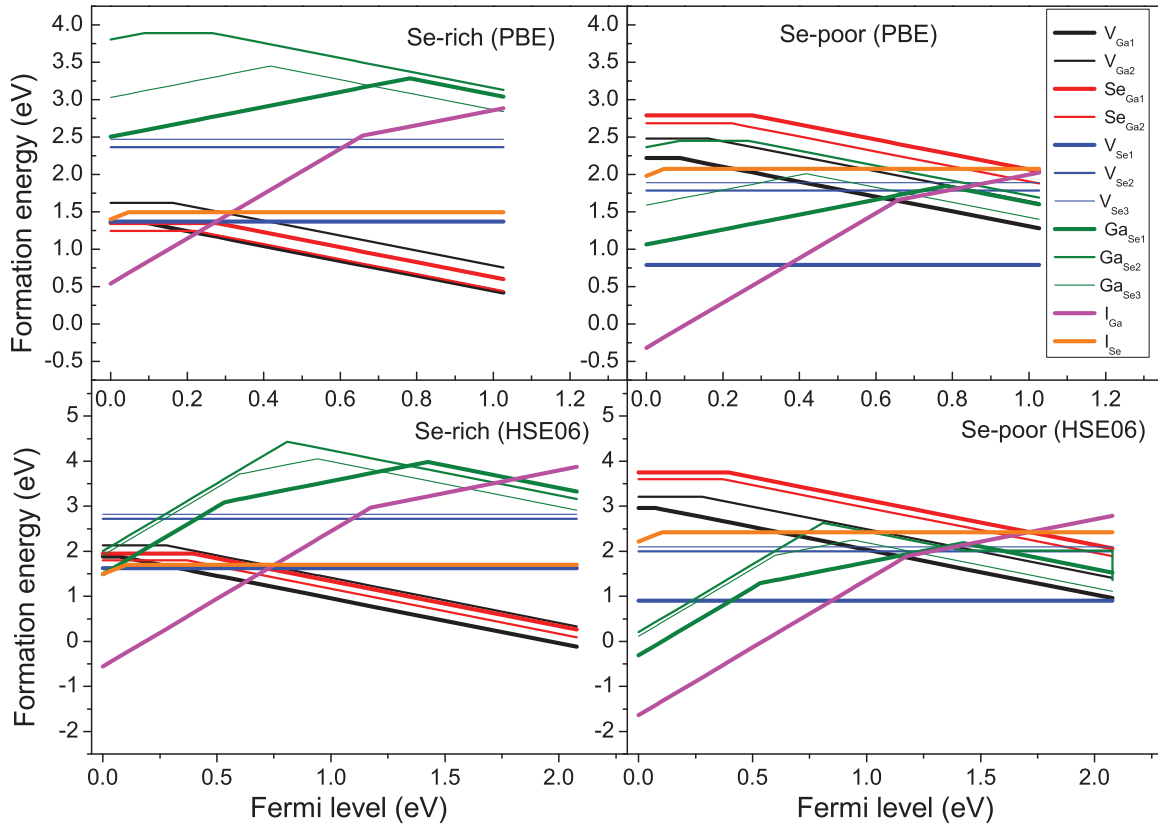


FIG. 5. (Color online) Formation energy of native point defects in mono- Ga_2Se_3 . Therein the periodic images interaction has been corrected for Ga interstitial. (The interaction of other defects is small, and not corrected.)

supercell. We can see that for I_{Ga}^{3+} in mono- or ortho- Ga_2Se_3 , the spurious interaction energy is about 0.30 eV for the small supercell, and for the other defects, the spurious interaction energy is less than 0.1 eV. For I_{Ga}^{1+} , although the influence of finite supercell size is small, the dependence on $1/N_{\text{cells}}$ is less clear. It may have something to do with the delocalized nature (as mentioned by Oba *et al.*⁶²) of the charged defect I_{Ga}^{1+} .

8. Formation energy of intrinsic point defects in mono- Ga_2Se_3

The calculated formation energy of intrinsic point defects as a function of Fermi level (electron chemical potential) based on PBE and HSE06 (PBE) is shown in Fig. 5, and the transition

levels are shown in Table III. The native point defects will be discussed one by one as follows:

(a) *The Ga vacancy ($V_{\text{Ga}1}$) is the only shallow acceptor.* The $V_{\text{Ga}1}$ is the only shallow acceptor in mono- Ga_2Se_3 (more or less deep). When the spurious effects of finite supercell are corrected, the transition level $\epsilon(0/-1)$ is 0.105 eV [HSE06(PBE)]. The transition levels of the other defects are larger than 0.27 eV [HSE06(PBE)]. However, LDA tends to predict a smaller transition level than PBE. The transition level $\epsilon(0/-1)$ of $V_{\text{Ga}1}$ is 0.054 eV for HSE06(LDA) with correction. According to the GW calculation results, the band gap is not fully reproduced by HSE06, so the actual transition level should be deeper than the calculated value of >0.11 eV for HSE06(PBE), or >0.05 eV for HSE06(LDA). It is unclear

TABLE III. Transition levels of native point defects of mono- Ga_2Se_3 (in eV). Therein the results of I_{Ga} are corrected. The charge transition levels are defined with respect to the VBM.

Supercell	k point		$V_{\text{Ga}1}$	$V_{\text{Ga}2}$	$\text{Se}_{\text{Ga}1}$	$\text{Se}_{\text{Ga}2}$	$\text{Ga}_{\text{Se}1}$	$\text{Ga}_{\text{Se}1}$	$\text{Ga}_{\text{Se}2}$	$\text{Ga}_{\text{Se}3}$	$\text{Ga}_{\text{Se}3}$	I_{Ga}
Transition level			(0/−1)	(0/−1)	(0/−1)	(0/−1)	(+1/−1)	(+3/+1)	(+3/−1)	(+1/−1)	(+3/+1)	(+3/+1)
232	111	LDA	0.035	0.074	0.129	0.077						0.705
	111	HSE06(LDA)	0.043									
	111	PBE	0.051	0.132	0.230	0.177	0.786			0.500		0.826
	111	HSE06(PBE)	0.073	0.277	0.394	0.368	1.426	0.533	0.808	0.938	0.601	1.174
	222	PBE	0.041	0.119	0.234	0.180						0.791
453	111	LDA	0.046									
	111	PBE	0.083	0.162	0.276	0.223	0.782			0.418		0.659

which predictions are more accurate, LDA or GGA(PBE), at present.

Under Se-rich conditions, the formation energy of neutral V_{Ga} is 1.36 eV (PBE) or 1.88 eV [HSE06(PBE)]. This indicates that the incorporation of nonlocal exchange would increase the calculated formation energy of neutral V_{Ga} [note that the transition level $\epsilon(0/-1)$ would be increased as well]. Alkauskas *et al.*⁵² assumed that the formation energy of neutral defect is insensitive to the fraction of nonlocal exchange. However, this is incorrect for Ga vacancy in Ga_2Se_3 . Due to the underestimation of the band gap, the actual formation energy of neutral V_{Ga} should be larger. According to Table II, under Se-poor conditions, the formation energy of Ga vacancy should increase by 0.86 eV (PBE) or 1.08 eV [HSE06(PBE)].

(b) *The Ga interstitial (I_{Ga}) is always a donor, in either +1 or +3 charge state.* As shown in Fig. 5, the Ga interstitial (I_{Ga}) is always a donor, in either +1 or +3 charge state. In fact, for the neutral Ga interstitial, one electron occupies the CBM. This indicates that one of the introduced defect levels by the Ga interstitial is above the CBM. We can compare the results with the Zn interstitial in ZnO.⁶¹ The transition level of $\epsilon(+2/0)$ for the Zn interstitial is slightly below the CBM as shown by Oba *et al.*⁶¹ The reason for this seems to be related to the adopted correction scheme of supercell size effects. As shown in Fig. 4, when the supercell effects are corrected, the formation energy of the charged defect would increase, which causes the transition level of $\epsilon(+1/0)$ to shift downwards. That is to say, the apparent stability of neutral charge state in the calculations of ZnO⁶¹ may be due to an artificial effect of the supercell size correction scheme. When the CBM is occupied by electrons, the neutral charge state should be unstable. Nevertheless, it may need further investigation.

Under Se-rich conditions, the formation energy of the Ga interstitial (I_{Ga}^{3+}) is negative [HSE06(PBE)] for an extremely p -type condition (E_F at E_{VBM}), as shown in Fig. 5. Further, the incorporation of nonlocal exchange would decrease the calculated formation energy of the Ga interstitial (I_{Ga}^{3+}). Due to the underestimation of the band gap (HSE06), the actual formation energy of the Ga interstitial (I_{Ga}^{3+}) should be lower. Under Se-poor conditions, the formation energy of the Ga interstitial should decrease by 0.86 eV (PBE) or 1.08 eV [HSE06(PBE)]. Although a negative formation energy is not entirely physical, such negative calculated values are not uncommon in the calculations of compound semiconductors.^{43,61} The removal of electrostatic interaction can increase the formation energy of I_{Ga}^{3+} by 0.34 eV, which has been already included in Fig. 5, which indicates that there exists attractive interaction between positively charged Ga interstitials, which is similar to the positively charged Zn interstitial in ZnO. This is also consistent with the commonly observed positive binding energy of di-interstitial atoms in metals,⁶³ which indicates that the elastic interaction should dominate the interactions between the interstitials in the short distance range. However, for sufficiently long distance interaction, the Coulomb interaction should dominate, and be repulsive. In experiments, annealing seems to decrease the lattice constant. This could be consistent with the removal of the Ga interstitial upon annealing.

Nevertheless, the formation energy of the Ga interstitial (I_{Ga}^{3+}) should be small under p -type conditions. A strong

compensation of holes by the Ga interstitial (I_{Ga}^{3+}) is expected in p -type Ga_2Se_3 . It should be difficult to dope mono- Ga_2Se_3 to get a high hole (p -type carrier) concentration, similar to ZnO.

It is unclear whether the low formation energy of the Ga interstitial is correlated with the growth condition of structural Ga vacancy ordering. According to Mikkelsen,⁶⁰ Ga-rich samples will not transform to the vacancy-ordered phase under any conditions. This could result from a large concentration of Ga interstitials in the Ga-rich samples. If this is indeed the case, then not only the chemical potential of Ga and Se but also the electron chemical potential (Fermi level) are important in determining the extent of vacancy ordering, because the Fermi level also has a large influence on the formation energy of the Ga interstitial. That is to say, the vacancy-ordered phase should be difficult to form under p -type and Ga-rich conditions, and easier to form under n -type and Ga-poor conditions. (Both n type and p type have been reported in the literature.^{19–22}) In this way, we can explain why the Ga/Se ratio can influence vacancy ordering. However, this should still be considered as inference, rather than a definite conclusion which requires further investigation. The measurement of lattice constants may be relevant to the problem, and could reveal whether there is an extensive concentration of Ga interstitials in the sample. In order to explain the necessity of Se-rich conditions for vacancy ordering, Mikkelsen⁶⁰ suggested that the reason why Ga-rich samples cannot transform to the vacancy-ordered phase is that it is more difficult to attain stoichiometry for Ga-rich samples than for Se-rich samples, which seems to imply that the diffusion of Ga interstitials is much more difficult than Se interstitials (based on the assumption that stoichiometry plays an important role in the vacancy ordering). This is supported by our migration barrier calculations for p -type conditions, as shown later. The migration barrier of Se interstitials is indeed much smaller than that of Ga interstitials under p -type conditions. On the other hand, under n -type conditions, both Ga and Se interstitials can diffuse fast, which may indicate that Ga-rich or Ga-poor should be irrelevant to vacancy ordering under n -type conditions.

In addition, we will discuss some additional detail of the Ga interstitial structure. For neutral and +1 charged defects, in fact, an off-site configuration in which the Ga atom is not at the structural vacancy site is more stable than the on-site configuration (with about 0.1 eV lower formation energy). This will be discussed further in the diffusion section. For the +3 charge state of the Ga interstitial (I_{Ga}), the Ga atom is almost at the center of the structural Ga vacancy site. For the +1 charge state, the Ga atom deviates from the structural Ga vacancy site to some extent, and it can transfer easily to a more stable off-site configuration. We can see that although they have different energies, the energy difference is small (about 0.1 eV). Due to the computational cost of hybrid DFT calculations, the off-site configuration has not been calculated, and the on-site configuration is used to represent the I_{Ga}^{1+} .

(c) *The Se vacancy is a neutral defect.* The Se vacancy is neutral over the whole range of the Fermi level, which is different from the oxygen vacancy in ZnO⁴³ or Te vacancy in GaTe.⁶⁴ The result is rather surprising. However, since this defect does not introduce a defect level in the band gap

(by checking the band structure), and the valence band is fully occupied, the neutral state should be the only stable state. Therefore this result should be reliable.

Umeda *et al.*⁶⁵ proposed that an antisite-vacancy pair can be more stable than the vacancy. The so-called antisite-vacancy pair means that a nearest-neighbor cation atom occupies the anion vacancy to form an antisite; together with the newly generated cation vacancy, it forms an antisite-vacancy pair. The anion vacancy and the cation AV counterparts may form a bistable defect pair. We have also checked this possibility by direct PBE calculations. For Ga_2Se_3 , the antisite-vacancy pair is not stable and it will transform to the configuration of the Se vacancy automatically, for various different charge states.

Under Se-rich conditions, the formation energy of the most stable neutral Se vacancy is 1.37 eV (PBE) or 1.62 eV [HSE06(PBE)]. Compared with the results of the Ga vacancy under an extremely p -type condition (E_F at E_{VBM}), we can see that using PBE, the Se vacancy has a slightly higher formation energy than the Ga vacancy by 0.01 eV, but based on HSE06(PBE) calculations, the Se vacancy has a lower formation energy than the Ga vacancy by 0.26 eV. According to Table II, under Se-poor conditions, the formation energy of the Se vacancy should decrease by 0.58 eV (PBE) or 0.72 eV [HSE06(PBE)]. Based on HSE06(PBE), the concentration of the Se vacancy should be larger than the Ga vacancy. Se vacancies are neutral defects, which do not contribute to the carrier concentration.

(d) *Se interstitials.* There are many possible configurations for Se interstitials. Some adopt a dumbbell interstitial configuration (or split interstitial), in which two Se atoms occupy one lattice site. However, for the most stable configuration, the Se interstitial atom stays between two Se(X) atoms, which will be described in more detail in the diffusion section later.

The Se interstitial is an anion interstitial, and is expected to be an acceptor, for example, the oxygen interstitial in ZnO ⁴³ and Te interstitial in GaTe .⁶⁴ However, the Se interstitial in Ga_2Se_3 seems to be special. As shown in Fig. 5, the Se interstitial is almost neutral over the whole range of the Fermi level, and is a donor under extremely p -type conditions (E_F at E_{VBM}). The result is surprising. However, this is similar to the oxygen dumbbell interstitial in ZnO ,⁴³ which is also neutral over the whole range of the Fermi level. We have also checked the possible configurations similar to the -2 charge state of the oxygen interstitial in ZnO , but find no new stable state.

Under Se-rich conditions, the formation energy of the most stable neutral Se interstitial is 1.49 eV (PBE) or 1.70 eV [HSE06(PBE)]. According to Table II, under Se-poor conditions, the formation energy of the Se interstitial should increase by 0.58 eV (PBE) or 0.72 eV [HSE06(PBE)].

(e) *The antisite defect Se_{Ga} is a deep acceptor.* It is expected that the Se_{Ga} antisite defect is an acceptor, similar to the O_{Zn} antisite defect in ZnO .⁴³ As shown in Fig. 5, the Se_{Ga} antisite is indeed an acceptor. It is similar to the Ga vacancy, presumably due to the neutral nature of the Se interstitial. However, Se_{Ga} possesses a deeper transition level than a Ga vacancy. In contrast, Te_{Ga} in GaTe ⁶⁴ can be either a donor or acceptor.

Under Se-rich conditions, the formation energy of the most stable neutral Se_{Ga} antisite defects is 1.24 eV (PBE) or 1.80 eV [HSE06(PBE)]. Compared with the results of the Ga vacancy under extremely p -type conditions (E_F at E_{VBM}), Se_{Ga} has

a slightly lower formation energy than V_{Ga} . According to Table II, under Se-poor conditions, the formation energy of the Se_{Ga} antisite defect should increase by 1.44 eV (PBE) or 1.80 eV [HSE06(PBE)].

(f) *The antisite defect Ga_{Se} is an acceptor under n -type conditions and a donor under p -type conditions.* The antisite defects Ga_{Se} can be a donor or an acceptor, as shown in Fig. 5. For HSE06, the $+3$ charge state is stable under p -type conditions, whereas the $+3$ charge state is not stable for PBE. The reason is that Ga_{Se} introduces one occupied level and one half-occupied level in the band gap for HSE06, but only one half-occupied level in the band gap for PBE. In addition, $\text{Ga}_{\text{Se}}^{3+}$ is actually not an on-site configuration (HSE06) and the Ga atom deviates severely from the Se site, and tends to occupy the structural vacancy site, which can be viewed as a $I_{\text{Ga}}V_{\text{Se}}$ complex. On the other hand, $\text{Ga}_{\text{Se}}^{1+}$ and Ga_{Se}^0 are more or less structurally consistent with an on-site configuration. Based on HSE06 calculations, the neutral state is unstable for Ga_{Se} .

Due to the high positive charge state, the formation energy of Ga_{Se} under extremely p -type conditions can be very low. Similar phenomena are also observed in ZnO , in which the Zn_{O} in ZnO has the lowest formation energy under extremely p -type and Zn-rich conditions.⁶¹ However, the low formation energy may be due to the negative formation energy of the Ga interstitial. Assuming positive formation energy of the Ga interstitial and Se vacancy, calculating the formation energy of Ga_{Se} based on binding energy between the Ga interstitial and Se vacancy should predict a much larger formation energy.

(g) *Formation energy of Frenkel-pair defect and binding energy of antisite defects.* The formation energy of the Frenkel-pair defect and binding energy of antisite defects based on both GGA and HSE06(GGA) are shown in Fig. 6. They are independent of the chemical potential of Ga and Se. However, they are dependent on the Fermi level (electron chemical potential). Under extremely p -type conditions (at VBM), the formation energy of the Frenkel-pair defect ($V_{\text{Ga}}-I_{\text{Ga}}$) is relatively small (1.3 eV) using HSE06(GGA). The formation energy of $V_{\text{Se}}-I_{\text{Se}}$ is larger than that of $V_{\text{Ga}}-I_{\text{Ga}}$ under p -type conditions, and smaller than that of $V_{\text{Ga}}-I_{\text{Ga}}$ under n -type conditions.

As shown in Figs. 6(c) and 6(d), the binding energy of $\text{Se}_{\text{Ga}1}$ (I_{Se} and $V_{\text{Ga}1}$ as the building unit) is about 1.5 eV using HSE06(GGA). This indicates that I_{Se} and $V_{\text{Ga}1}$ have a relatively large attractive interaction. For $\text{Ga}_{\text{Se}1}$, we can see that under p -type conditions, the binding energy is negative, which indicates that I_{Ga} and $V_{\text{Se}1}$ have a repulsive interaction. This indicates that $\text{Ga}_{\text{Se}1}$ is not easy to form. The low formation energy of $\text{Ga}_{\text{Se}1}$ seems to be due to the large negative formation energy of the Ga interstitial under extremely p -type conditions. On the other hand, under n -type conditions (at CBM), the binding energy is positive (attractive interaction).

9. Comparison of transition levels between PBE and HSE

As shown in Table VI, except for $V_{\text{Ga}1}$ and I_{Ga} , the transition levels calculated by HSE06(PBE) tend to be about twice those of PBE, close to the ratio of calculated band gaps (2.09 eV vs 1.05 eV). The transition level as a function of mixing ratio (AEXX) seems to be almost linear. Such linear behaviors have been observed by Alkauskas *et al.*⁵² for Si and have

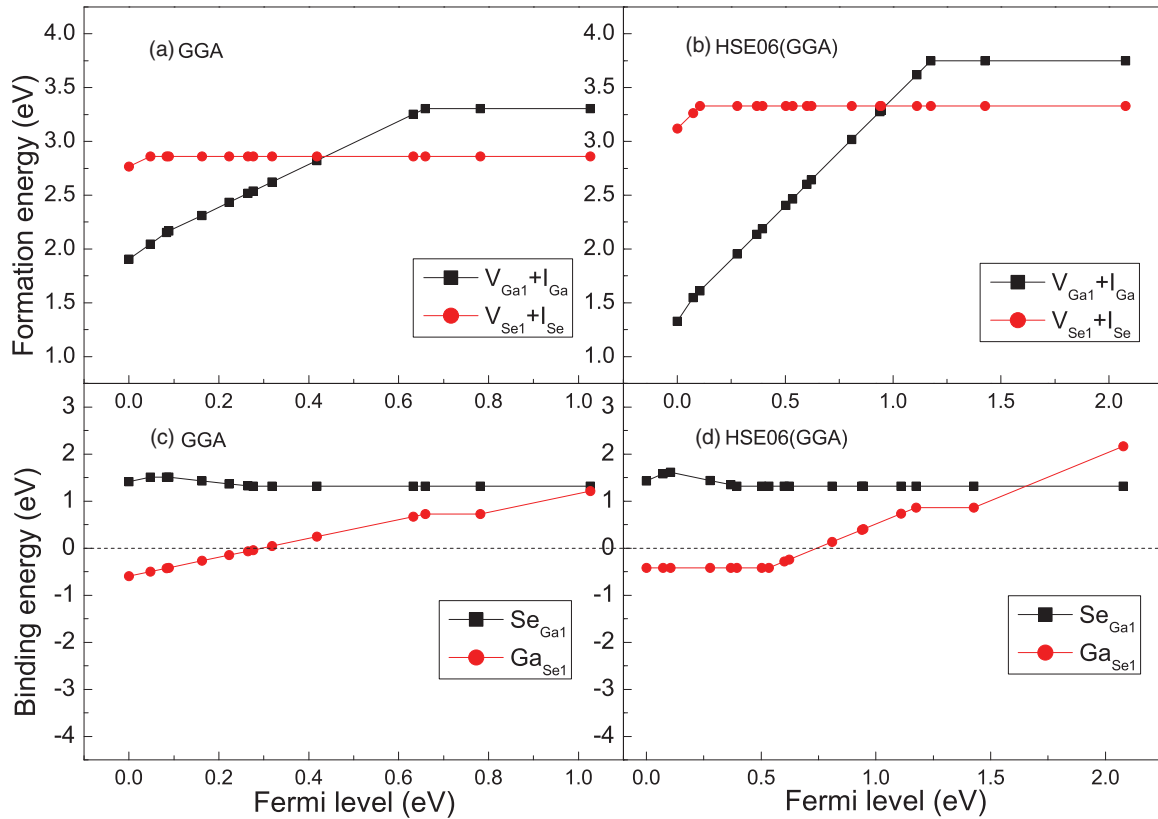


FIG. 6. (Color online) Formation energy of Frenkel-pair defect and binding energy of antisite defects in mono-Ga₂Se₃. Positive binding energy indicates attractive interaction, and negative binding energy indicates repulsive interaction.

also been observed in ZnO using the LDA + U correction method.⁵⁴

According to Alkauskas *et al.*,⁵² the transition level of well-localized midgap states with respect to the average electrostatic potential is insensitive to the mixing ratio (AEXX). As shown in Fig. 2, the electrostatic potential is insensitive to the mixing ratio (AEXX), so the transition level with respect to the average electrostatic potential corresponds to the absolute value of the transition level, which is equal to VBM + transition level. The calculation results are shown in Fig. 7. This shows that when the transition level is at the middle of the band gap, it is insensitive to the mixing ratio (AEXX). That is to say,

the observation of Alkauskas *et al.*⁵² is supported by our calculations.

C. Native point defects in ortho-Ga₂Se₃

The calculated formation energy of native point defects in ortho-Ga₂Se₃ as a function of Fermi level (electron chemical potential) based on PBE and HSE06 (PBE) calculations is shown in Fig. 8, and the transition levels are shown in Table IV.

(a) Both Ga vacancy (V_{Ga}) and antisite defect Se_{Ga} are shallow acceptors. Different from the mono-Ga₂Se₃, both the Ga vacancy (V_{Ga}) and antisite defect Se_{Ga} in ortho-Ga₂Se₃ are shallow acceptors. Therein the antisite defect Se_{Ga} has a shallower transition level than the Ga vacancy (V_{Ga}), which is supported by both LDA and GGA calculations, although Se_{Ga} has a larger formation energy than V_{Ga} . The transition level $\epsilon(0/-1)$ of Se_{Ga} and V_{Ga} is 0.047 eV and 0.074 eV for HSE06(PBE) with the correction of size effect, respectively. It should be noted that LDA calculations tend to predict a smaller transition level than GGA, similar to mono-Ga₂Se₃.

Under Se-rich conditions, the formation energy of neutral V_{Ga1} is 0.79 eV (PBE) or 1.31 eV [HSE06(PBE)]. This indicates that the incorporation of nonlocal exchange would increase the calculated formation energy of neutral V_{Ga1} [and also the transition level $\epsilon(0/-1)$]. Compared with the corresponding formation energy in mono-Ga₂Se₃, we can see that the formation energy of Ga vacancy is lower in ortho-Ga₂Se₃. It seems that the concentration of p -type carrier should be higher in ortho-Ga₂Se₃ than in mono-Ga₂Se₃

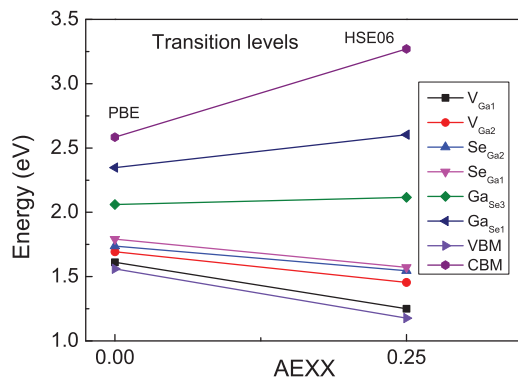


FIG. 7. (Color online) Absolute transition levels as a function of mixing ratio (AEXX) in mono-Ga₂Se₃.

TABLE IV. Transition levels of native point defects of ortho-Ga₂Se₃ (in eV). Therein the results of I_{Ga} are corrected. The charge transition levels are defined with respect to the VBM.

Supercell	k point		V_{Ga}	Se_{Ga}	$\text{Ga}_{\text{Se}1}$	$\text{Ga}_{\text{Se}2}$	I_{Ga}
Transition level			(0/−1)	(0/−1)	(0/−1)	(0/−1)	(+3/+1)
264	111	LDA	0.017	0.001	0.326	0.043	0.453
	111	PBE	0.025	0.004	0.435	0.046	0.322
	111	HSE06(PBE)	0.050	0.018	0.680	0.111	0.983
396	111	PBE	0.049	0.033	0.504	0.059	0.404

(when the compensation defects are not considered). According to Table II, under Se-poor conditions, the formation energy of the Ga vacancy should increase by 0.86 eV (PBE) or 1.08 eV [HSE06(PBE)].

(b) *The Ga interstitial (I_{Ga}) is always a donor, either in the +1 or +3 charge state.* As shown in Fig. 8, the Ga interstitial (I_{Ga}) is always a donor, either in the +1 or +3 charge state, similar to mono-Ga₂Se₃.

Under Se-rich conditions, the formation energy of the Ga interstitial (I_{Ga}^{3+}) is small [HSE06(PBE)] for extremely p -type conditions (E_F at E_{VBM}). Under Se-poor conditions, the formation energy of the Ga interstitial should decrease by 0.86 eV (PBE) or 1.08 eV [HSE06(PBE)]. Compared with the corresponding results of mono-Ga₂Se₃, the formation energy of the Ga interstitial is higher in ortho-Ga₂Se₃.

(c) *Se vacancy.* As shown in Fig. 8, the Se vacancy is neutral over the whole range of the Fermi level. This result is similar to that of mono-Ga₂Se₃.

Under Se-rich conditions, the formation energy of the most stable neutral Se vacancy is 1.25 eV (PBE) or 1.44 eV [HSE06(PBE)]. Under Se-poor conditions, the formation energy of the Se interstitial should decrease by 0.58 eV (PBE) or 0.72 eV [HSE06(PBE)], respectively. Compared with the corresponding results of mono-Ga₂Se₃, the formation energy of the Se vacancy is lower in ortho-Ga₂Se₃.

(d) *Se interstitial.* As shown in Fig. 8, the Se interstitial is neutral over the whole range of the Fermi level. The results are similar to those of mono-Ga₂Se₃. The Se interstitial adopts a dumbbell interstitial configuration, which will be described in the diffusion section. Under Se-rich conditions, the formation energy of the most stable neutral Se interstitial is 1.13 eV (PBE) or 1.39 eV [HSE06(PBE)]. Under Se-poor conditions, the formation energy of Se interstitial should increase by 0.58 eV (PBE) or 0.72 eV [HSE06(PBE)], respectively. Compared with the corresponding results of mono-Ga₂Se₃, the formation energy of the Se interstitial is lower in ortho-Ga₂Se₃.

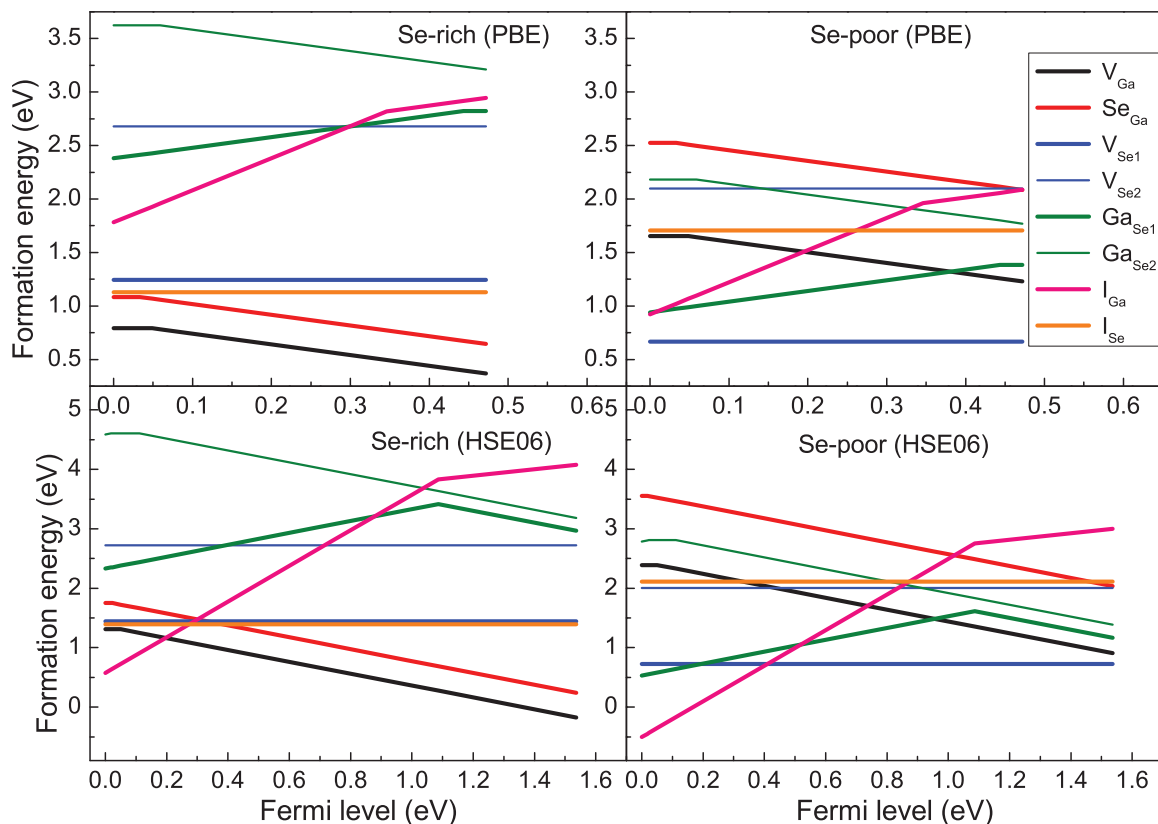


FIG. 8. (Color online) Formation energy of native point defects in ortho-Ga₂Se₃. Therein the periodic images interaction has been corrected for I_{Ga}^{3+} .

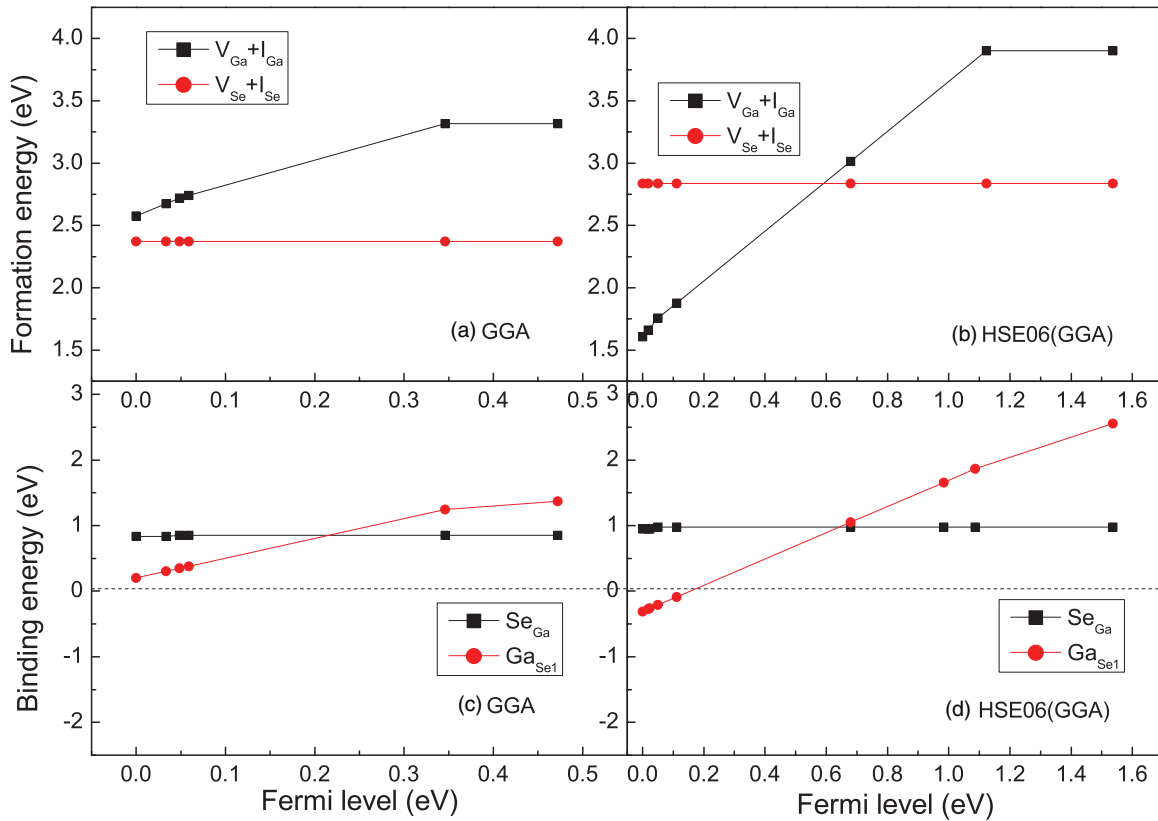


FIG. 9. (Color online) Formation energy of Frenkel-pair defect and binding energy of antisite defects in ortho-Ga₂Se₃.

(e) The antisite defect Ga_{Se} is an acceptor under n -type conditions and a donor under p -type conditions. The antisite defect Ga_{Se} can be a donor or acceptor, as shown in Fig. 8. Different from the mono-Ga₂Se₃, this result indicates that Ga_{Se} may play an important role in Se-poor conditions.

(f) Formation energy of the Frenkel-pair defect and binding energy of antisite defects. The formation energy of the Frenkel-pair defect and binding energy of antisite defects, based on both GGA and HSE06(GGA) calculations, are shown in Fig. 9. They are independent of the chemical potential of Ga and Se, but are dependent on the Fermi level (electron chemical potential). Under extremely p -type conditions (at VBM), the formation energy of the Frenkel-pair defect ($V_{Ga}-I_{Ga}$) is relatively small (1.5 eV) using HSE06(GGA), larger than that of mono-Ga₂Se₃. The formation energy of $V_{Se}-I_{Se}$ is larger than that of $V_{Ga}-I_{Ga}$ under p -type conditions, and smaller than that of $V_{Ga}-I_{Ga}$ under n -type conditions (HSE06).

As shown in Figs. 9(c) and 9(d), the binding energy of Se_{Ga1} (I_{Se} and V_{Ga1} as the building unit) is 1.0 eV for HSE06(GGA). This indicates that I_{Se} and V_{Ga1} have a relatively large attractive interaction. For Ga_{Se1} , we can see that under p -type conditions, the binding energy is negative, which indicates that I_{Ga} and V_{Se1} have a repulsive interaction. This indicates that Ga_{Se1} is not easy to form under extremely p -type conditions. The low formation energy of Ga_{Se1} seems to be due to the large negative formation energy of the Ga interstitial under extremely p -type conditions. On the other hand, under n -type conditions (at CBM), the binding energy is positive (attractive interaction).

1. Comparison with experiments

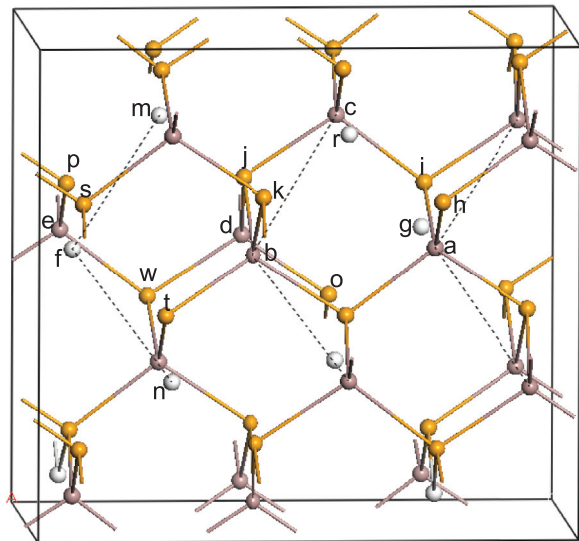
According to the calculation results, Ga₂Se₃ should be p type under Se-rich conditions and n type under Se-poor conditions. The concentration of charge carriers (holes or electrons) is predicted to be low under both Se-rich and Se-poor conditions. In the literature, both p -type^{20–22} and n -type¹⁹ conductivities have been reported for the undoped Ga₂Se₃. Based on the calculations, without doping, the concentration of charge carriers cannot be high under any equilibrium condition. Under Se-rich conditions, the concentration of holes in ortho-Ga₂Se₃ is higher than that of mono-Ga₂Se₃.

IV. DIFFUSION BEHAVIORS OF NATIVE POINT DEFECTS

A. Native point defects in mono-Ga₂Se₃

1. Diffusion of Ga interstitial I_{Ga}

The Ga interstitial is expected to diffuse fast in Ga₂Se₃. As shown in Fig. 10, the Ga interstitial I_{Ga} can diffuse along the channel created by the zigzag line vacancies ($n \rightarrow f \rightarrow m$). For 0 and +1 charge state, there is a more stable off-site configuration for the Ga interstitial, with 0.096 eV and 0.103 eV lower energy, respectively. In order to diffuse along the zigzag line of vacancies channel, the atom has to transform from the on-site configuration to the off-site configuration, and then to the on-site configuration of a neighboring structural vacancy. The energy barrier that the on-site configuration transforms to the off-site configuration is 0.18 eV for both 0 and +1 charge state. The energy barrier that the off-site configuration transforms to a neighboring on-site


 FIG. 10. (Color online) Diffusion paths in mono-Ga₂Se₃.

configuration along the zigzag line of vacancies channel is 0.26 eV for both 0 and +1 charge state. That is to say, the Ga interstitial of 0 and +1 charge state diffuses along the channels created by zigzag line vacancies with 0.26 eV overall migration barrier. The +1 charge state is the stable charge state under *n*-type conditions. The neutral charge state is unstable; however, it is included for completeness. We can see that the Ga interstitial can diffuse very fast along the vacancy channel under *n*-type conditions, with 0.26 eV migration barrier.

For the +2 charge state, the off-site configuration is unstable, with 0.465 eV higher energy and a 0.089 eV energy well. The Ga interstitial of the +2 charge state diffuses along the zigzag line of vacancies with 0.55 eV migration barrier. The +2 charge state of the Ga interstitial is unstable throughout the whole range of Fermi levels. However, it has been included for completeness.

For the +3 charge state, the off-site configuration is unstable, and the interstitial transforms to the on-site configuration automatically during structure optimization. For the +3 charge state, the Ga interstitial atom is almost in the center of the structural vacancy, different from the +1 charge state. The Ga interstitial of the +3 charge state diffuses along the zigzag line of vacancies with a 1.25 eV migration barrier. The +3 charge state is stable under *p*-type conditions. We can see that under *p*-type conditions, the Ga interstitial diffuses much slower than *n*-type conditions. The off-site configuration does not introduce any defect level in the band gap, and the CBM is occupied by one electron. Therefore, it is expected that its +2 and +3 charge states of the Ga interstitial are unstable, which are not actually calculated.

As shown in Fig. 10, the Ga interstitial I_{Ga} can also diffuse directly to a neighbor zigzag line of vacancies ($g \rightarrow f$), with >1.2 eV migration barrier. The migration barriers are summarized in Table V.

For the diffusion between neighboring channels of zigzag line vacancies, the Ga interstitial I_{Ga} can also kick the neighbor Ga atoms to the neighbor zigzag line of vacancies. There are three possible paths, $a \rightarrow g \rightarrow a'$, $f \rightarrow a \rightarrow g$,

 TABLE V. Migration barrier of native point defects in mono-Ga₂Se₃ (in eV). The values in the brackets are the migration barrier of the corresponding reverse process.

Path		-1	0	+1	+2	+3
V_{Ga}	ab	1.84(1.52)	1.53(1.29)			
	cb	1.43(1.11)	1.06(0.81)			
	bd	1.39	1.47			
	ae	1.41	1.92			
	ac	1.61	1.62			
	aa'	2.79	2.80			
V_{Se}	ho	1.54	2.04	2.02		
	hp		3.06			
	hi		2.83(1.94)			
I_{Ga}	fm		0.26	0.26	0.55	1.25
	aga'		0.87	1.28	1.47	1.36
	gf		1.27	1.29	1.57	2.31
	fac		1.09	1.17	1.72	1.80
	fbr		0.97	1.21	1.38	1.73
I_{Se}	Zagzig:kick-out		0.17		0.68	
	Zagzig:interstitial		0.61			
	Between zigzag		0.65			
	Rotation		0.40			

and $f \rightarrow b \rightarrow r$. The migration barriers are summarized in Table V (>1.1 eV).

In summary, under *n*-type conditions (+1 charge state), The Ga interstitial can diffuse fast along zigzag lines of vacancies with a 0.26 eV migration barrier, and diffuses relatively slowly between zigzag lines of vacancies with 1.21 eV. Under *p*-type conditions (+3 charge state), the Ga interstitial diffuses along zigzag lines of vacancies with a 1.25 eV migration barrier, and diffuses between zigzag line vacancy channels with a 1.36 eV migration barrier. The results are more or less surprising, and indicate that under *p*-type conditions, the high radiation stability may be absent. Whether Ga₂Se₃ has high radiation stability under *p*-type conditions may need further investigations, although the In₂Te₃ has been observed to have high radiation stability.¹⁻³

2. Diffusion of Se interstitial I_{Se}

The Se interstitial is also expected to diffuse fast in Ga₂Se₃. In order to describe the diffusion of the Se interstitial, it is necessary to describe the Se interstitial structure in more detail. According to Newman,³⁰ each vacancy is surrounded by two Se(X) and two Se(Y) atoms. When a Se atom is inserted into the structural vacancy site, it will relax to the midpoint between the two neighboring Se(X) atoms, and the two Se(X) atoms will be pushed slightly off-site away from the inserted Se atoms. Figure 10 shows the configurations when inserting a Se atom on site f ; it will relax to the midpoint between site p and site t . This structure is the most stable configuration for the neutral Se interstitial (there are many metastable configurations for the Se interstitial), and is an important configuration for Se interstitial diffusion. It is important to identify this structure; otherwise it is difficult to find out the small migration barrier path along the channel created by zigzag-line vacancies. The vacancies in mono-Ga₂Se₃ are in a zigzag-line form, as shown in Fig. 10 ($n \rightarrow f \rightarrow m$), and the

Se(X) atoms in the continuous vacancy-Se(X) chain also adopts a zigzag-line form.³⁰ The Se interstitial can diffuse along the zigzag-line vacancy channel by an interstitial mechanism or kick-out mechanism [the Se interstitial does not actually stay in the structural vacancy site, but stays between two Se(X) atoms along the zigzag-line Se(X) chain]. That is to say, the diffusion of the Se interstitial along the zigzag-line vacancy channel can also be viewed as diffusion along the zigzag-line Se(X) chain. Therefore, the kick-out mechanism is the natural mechanism based on a structural consideration. Indeed, the migration barrier for the kick-out mechanism [Se interstitial kicks neighboring Se(X) to interstitial site] along the zigzag-line Se(X) chain for a neutral Se interstitial [Se interstitial stays in the middle of two neighboring Se(X) atoms in the zigzag-line chain] is very small (0.17 eV). On the other hand, the +2 charge state of the Se interstitial (the structure is similar) is more stable under extremely *p*-type conditions, for which the migration barrier is relatively large (0.68 eV). On the other hand, the migration barrier for the interstitial mechanism (the Se interstitial transforms to a neighbor interstitial site directly) of a neutral Se interstitial is much larger (0.61 eV) than the kick-out mechanism. (Diffusion for +2 charge state via interstitial mechanism is not calculated.)

For the diffusion of the Se interstitial between neighboring channels of zigzag-line vacancies, the migration path is complicated. There are numerous possible migration paths, and several metastable configurations are present in the migration path. However, only some of them are the limiting process. Most of the metastable configurations of the Se interstitial involve a dumbbell interstitial (two atoms occupying one lattice site). The rotation of the dumbbell interstitial at one lattice site is about 0.4 eV. The migration barrier between the neighboring zigzag-line vacancy channel for the neutral Se interstitial is about 0.65 eV. Since only some of the migration paths and some part of the migration paths are calculated, the results presented here are necessarily incomplete and may not be so reliable. More precise results would require further investigation.

In summary, the Se interstitial can diffuse very fast along the vacancy channel except under extremely *p*-type conditions, which can explain the high radiation stability of Ga₂Se₃.

3. Diffusion of Ga vacancy V_{Ga} and Se vacancy V_{Se}

Diffusion of the Ga vacancy and Se vacancy are well defined. There is no need to describe the migration path. The results are summarized in Table V. The Ga vacancy diffuses relatively slowly, with >1.0 eV migration barrier. The Se vacancy diffuses more slowly than the Ga vacancy, with >2.0 eV migration barrier. The diffusion paths for the Se vacancy have not been fully calculated here, but the remaining migration barriers should be similar.

B. Native point defects in ortho-Ga₂Se₃

1. Diffusion of Ga interstitial I_{Ga}

The Ga interstitial can diffuse along the straight-line vacancy channel ($a \rightarrow b$). Under *n*-type conditions (+1 charge state), the migration barrier is 0.19 eV. Under *p*-type conditions (+3 charge state), the migration barrier is 0.97 eV.

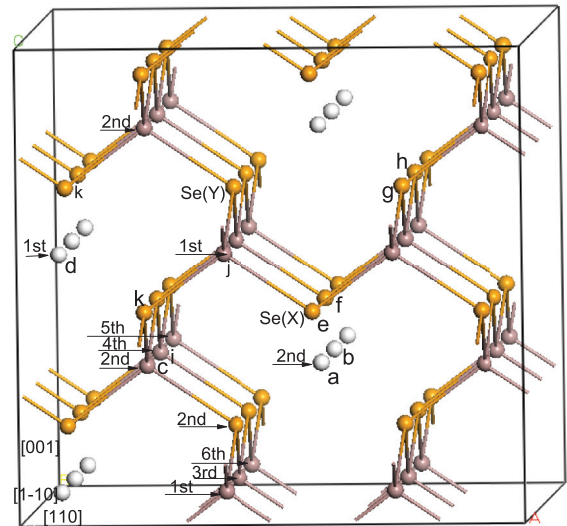


FIG. 11. (Color online) Diffusion paths in ortho-Ga₂Se₃.

Similarly to mono-Ga₂Se₃, the Ga interstitial diffuses fast under *n*-type conditions, but diffuses much more slowly under *p*-type conditions.

It is necessary to point out that for the neutral charge state, the off-site configuration is more stable, with 0.08 eV lower energy. The Ga interstitial atom in the off-site configuration is almost below the Se atom (*e*) (with almost the same *x* and *y* coordinates) as shown in Fig. 11. For the +1 charge state, the off-site configuration has 0.07 eV higher energy. For the +2 and +3 charge state, the off-site configuration is unstable, with about 0.1 eV energy well.

It is much more difficult that the Ga interstitial diffuses between neighboring channels of straight-line vacancies ($a \rightarrow d$ and $a \rightarrow c \rightarrow d$), with a >1.5 eV migration barrier. The calculation results are summarized in Table VI.

2. Diffusion of Se interstitial I_{Se}

The Se interstitial in ortho-Ga₂Se₃ adopts the so-called dumbbell interstitial configuration. For the most stable configuration, the direction of the dumbbell interstitial (two Se atoms) is parallel to the straight-line vacancy channel. The *x*

TABLE VI. Migration barrier of native point defects of ortho-Ga₂Se₃ (in eV). The values in the brackets are the migration barrier of the corresponding reverse process.

Path		-1	0	+1	+2	+3
V_{Ga}	<i>ci</i>	0.84	0.92			
	<i>cj</i>	1.88	1.71			
V_{Se}	<i>ef</i>		1.79			
	<i>eg</i>		1.94(0.52)			
I_{Ga}	<i>ab</i>		0.12	0.19	0.59	0.97
	<i>ad</i>		1.34	1.52	1.92	2.31
	<i>acd</i>		1.26	1.61	2.00	2.39
I_{Se}	<i>ef</i>		0.18			
	<i>ek</i>		1.58			
	<i>akd</i>		1.07			

and z coordinates are almost unchanged, and almost the same as that of the corresponding Se lattice site. The migration barrier of the dumbbell Se interstitial along the straight-line vacancy channel is very small, 0.18 eV. The migration barrier of the dumbbell Se interstitial between different straight-line vacancy channels is much larger, >1.0 eV. The calculation results are summarized in Table VI.

3. Diffusion of V_{Ga} and V_{Se}

Diffusion of the Ga vacancy and Se vacancy in ortho- Ga_2Se_3 is well defined. And again, there is no need to describe the migration path here. The results are summarized in Table VI. The Ga vacancy diffuses relatively slowly, with >0.8 eV migration barrier. The Se vacancy diffuses more slowly than the Ga vacancy, with >1.3 eV migration barrier.

V. ANALYSIS OF THE DEFECT STATES

The introduction of point defects would unavoidably change the band structure of the perfect crystal. Generally speaking, point defects can introduce some new defect states in the forbidden band gap, or introduce resonant states in the valence bands or conduction bands. For a sufficiently large supercell, the VBM and CBM may be nearly not influenced by the defect states or resonant states. When adding or removing an electron to or from the supercell, if the band structure is almost not changed, the resulting energy difference should be equal to the corresponding energy level (becomes occupied or unoccupied). According to our calculations, for a sufficiently large supercell, the ionization potential I and electron affinity A are approximately equal to the VBM and CBM, respectively. (The definition is not repeated here; see Sec. III A in Ref. 44.) Our calculations confirmed the observation of Lany *et al.*⁴⁴ that the difference between the ionization potential I and the electron affinity A is converged to the calculated band gap, for a sufficiently large supercell. However, when the defect levels in the forbidden band gap become occupied or unoccupied, their positions can often change a lot, partially due to the atomic structure relaxation. For example, when the defect level of the oxygen vacancy in ZnO becomes unoccupied, it will be shifted upward significantly. (See Fig. 3 in Ref. 62.) Therefore, the introduced defect level in the band gap is often not directly related to the (thermodynamic) charge transition level, unless the introduced defect level is almost not shifted after the ionization; for example, the defect level of $\text{Se}_{\text{Ga}3}$ in mono- Ga_2Se_3 only changes slightly after becoming occupied, where its defect level is about 0.21 eV above VBM, close to the (thermodynamic) charge transition level (0.19 eV).

It is rather surprising that the anion vacancy in Ga_2Se_3 is neutral over the whole range of Fermi level (electron chemical potential), which is also true for Ga_2S_3 and Ga_2Te_3 based on our calculations using the same crystal structure. This seems to be the common character of the defect zinc blende A_2B_3 type III-VI compound semiconductor. Such behaviors were never observed for IV, III-V, II-VI group semiconductors. For the layered GaTe semiconductor,⁶⁴ its anion vacancy is not neutral over the whole range of electron chemical potential, but is a deep single donor. So it may be necessary to investigate the Se vacancy in more detail. First, we noticed that anion

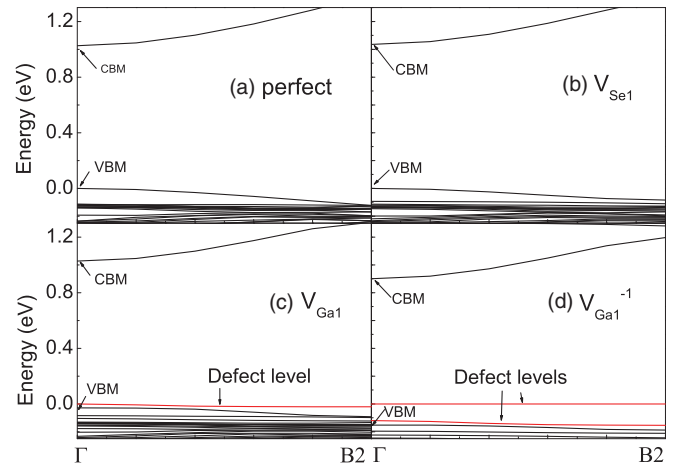


FIG. 12. (Color online) Band structure of mono- Ga_2Se_3 . (a) Perfect supercell. (b) Se vacancy. (c) Neutral charge state of Ga vacancy. (d) -1 charge state of Ga vacancy. The highest occupied energy level is shifted to 0.

(O, S, and Se) vacancy in the II-VI group semiconductors (ZnO ,^{43,62} ZnS ,^{66,67} and ZnSe ⁶⁸) introduced a deep fully occupied defect level (two electrons) in the band gap. (Therein, the Se vacancy in ZnSe is also a double acceptor under n -type conditions, which is surprising and indicates that it introduces a fully unoccupied defect level in the band gap at the same time, besides a fully occupied defect level.) For the neutral anion vacancy in II-VI group semiconductors, there is an inward relaxation around the vacancy,^{43,62,66–68} whereas for the $+2$ charge state, there is a large outward relaxation around the vacancy, where the vacancy defect level in the band gap becomes fully unoccupied. This indicates that the two localized electrons (occupying the deep defect level) are related to the inward relaxation around the vacancy. For the Se vacancy in Ga_2Se_3 , the neutral Se vacancy also has a large inward relaxation around the vacancy, (which should be responsible for the large migration barrier, similar to the oxygen vacancy in ZnO ⁴²). (In Se bonding with two or three Ga atoms, after removing the Se atom, the original bonding Ga will move towards the Se vacancy noticeably.) Second, there is no defect level in the band gap, as shown in Fig. 12(b). Therefore, we should infer that the Se vacancy in Ga_2Se_3 should also introduce a fully occupied defect level, which is below the VBM (a resonant state). If the Se vacancy introduces a half-occupied defect level, even if it is below the VBM, the VBM cannot be fully occupied. So it should be reliable that the anion vacancy in Ga_2Se_3 is neutral over the whole range of the Fermi level.

For the Ga interstitial, this introduces a fully occupied defect level in the band gap, and a half-occupied resonance above the CBM, where the electron of the resonance has transferred to the CBM. (The band structure is not shown here.) This is consistent with the Ga interstitial always being a donor, either with the $+3$ charge state or $+1$ charge state.

In addition, we also discuss further the defect calculations. The band structures of the neutral and -1 charge state Ga vacancy are shown in Figs. 12(c) and 12(d), respectively. The defect level of the neutral Ga vacancy is half occupied. Therein the band gap (CBM-VBM) is close to the band gap

of the perfect supercell. When the defect level becomes fully occupied, it is shifted upwards slightly, and an extra defect level above the VBM is generated (the red line). The reason we do not regard the second red line as the VBM is that if it is adopted as the VBM, the band gap is not close to the band gap of the perfect supercell any longer. Such behaviors are also common for the other defects. It is one main reason that previous authors believed the defect influences the VBM severely. Once an appropriate defect level is adopted as the VBM, the band gap is almost the same as the band gap of the perfect supercell. We also noticed that both the VBM and CBM are shifted slightly due to the influence of the defect, but the band gap (CBM-VBM) is relatively insensitive to the defect and its charge state.

VI. CONCLUSION

Based on first-principles calculations, we have performed a comprehensive and systematic investigation of the energetics and kinetics of native point defects in Ga₂Se₃.

The Ga vacancy and antisite defect Se_{Ga} are the two possible shallow acceptors in Ga₂Se₃. The Ga interstitial is always a donor, either with the +3 charge state under *p*-type conditions

or the +1 charge state under *n*-type conditions. Both the Se vacancy and Se interstitial are neutral defects except under the extremely *p*-type condition for the Se interstitial.

As expected, both the Ga interstitial and Se interstitial are predicted to be a very fast diffuser under *n*-type conditions, with a <0.3 eV migration barrier. However, quite unexpectedly under *p*-type conditions, the calculated migration barrier of the Ga interstitial is relatively large, >1.0 eV. The +2 charge state is stable for the Se interstitial under extremely *p*-type conditions. The migration barrier of the +2 charge state of a Se interstitial is relatively large, 0.68 eV. The migration barriers of the Ga vacancy and Se vacancy are >0.8 eV and >1.3 eV, respectively.

ACKNOWLEDGMENTS

The authors would like to acknowledge N. M. Abdul-Jabbar (UC Berkeley) for many motivating discussions. This research has been funded by the US Department of Energy, Office of Nuclear Energy, through the Nuclear Energy University Program, administered by Batelle Energy Alliance, LLC, Subcontract No. 00091204, CFDA No. 81.049, and partially as part of the DHS-NSF Academic Research grant at the University of California, Berkeley.

*huangguiyang@gmail.com

†bdwirth@utk.edu

¹V. M. Koshkin, L. P. Gal'chinskii, V. N. Kulik, and B. I. Minkov, *Solid State Commun.* **13**, 1 (1973).

²V. M. Koshkin, L. P. Gal'chinskii, V. N. Kulik, and U. A. Ulmanis, *Radiat. Eff.* **29**, 1 (1976).

³Y. G. Gurevich, V. M. Koshkin, and I. N. Volovichev, *Solid-State Electron.* **38**, 235 (1995).

⁴N. A. Goryunova, V. S. Grigor'eva, B. M. Konovalenko, and S. M. Ryvkin, *Zh. Tekh. Fiz. (Moscow)* **25**, 1675 (1955).

⁵J. C. Woolley and B. Ray, *J. Phys. Chem. Solids* **16**, 102 (1960).

⁶S. Sen and D. N. Bose, *Solid State Commun.* **50**, 39 (1984).

⁷K. Wuyts, J. Watt, G. Langouche, R. E. Silverans, G. Zégbé, and J. C. Jumas, *J. Appl. Phys.* **71**, 744 (1992).

⁸C. Julien, I. Ivanov, C. Ecrepont, and M. Guittard, *Phys. Status Solidi A* **145**, 207 (1994).

⁹A. E. Bekheet, *Eur. Phys. J. (Appl. Phys.)* **16**, 187 (2001).

¹⁰G. A. Gamal, M. M. Abdalrahman, M. I. Ashraf, and H. J. Eman, *J. Phys. Chem. Solids* **66**, 1 (2005).

¹¹K. H. Park, H. G. Kim, W. T. Kim, C. D. Kim, H. M. Jeong, K. J. Lee, and B. H. Lee, *Solid State Commun.* **70**, 971 (1989).

¹²I. H. Mutlu, M. Z. Zarbaliyev, and F. Aslan, *J. SolCGel. Sci. Technol.* **50**, 271 (2009).

¹³J. Woolley and B. A. Smith, *Proc. Phys. Soc. (London)* **72**, 867 (1958).

¹⁴M. Kerkhoff and V. Leute, *J. Alloys Compd.* **381**, 124 (2004).

¹⁵W. W. Warren, Jr., G. F. Brennert, E. Buehler, and J. H. Wernick, *J. Phys. Chem. Solids* **35**, 1153 (1974).

¹⁶N. M. Abdul-Jabbara, E. D. Bourret-Courchesne, and B. D. Wirth, *J. Cryst. Growth* **352**, 31 (2012).

¹⁷G. Y. Huang, N. M. Abdul-Jabbar, and B. D. Wirth, *J. Phys.: Condens. Matter* **25**, 225503 (2013).

¹⁸Ga₂Se₃ crystal structure, lattice parameters, physical properties. O. Madelung, U. Rossler, and M. Schulz, eds., SpringerMaterials: The Landolt-Börnstein Database, <http://www.springermaterials.com>.

¹⁹D. I. Bletskan, V. N. Kabatsii, and M. Kranjcec, *Inorg. Mater.* **46**, 1290 (2010).

²⁰A. E. Belal, H. A. El-Shaikh, and I. A. Ashraf, *Cryst. Res. Technol.* **30**, 135 (1995).

²¹G. A. Gamal and H. A. El-Shaikh, *Cryst. Res. Technol.* **30**, 867 (1995).

²²M. Rusu, S. Wiesner, S. Lindner, E. Strub, J. Rohrich, R. Würz, W. Fritsch, W. Bohne, Th. Schedel-Niedrig, M. Ch. Lux-Steiner, Ch. Giesen, and M. Heuken, *J. Phys.: Condens. Matter* **15**, 8185 (2003).

²³M. Abdal-Rahman and H. A. El Shaikh, *J. Phys.* **29**, 889 (1996).

²⁴G. Kresse and J. Hafner, *Phys. Rev. B* **47**, 558 (1993).

²⁵G. Kresse and J. Furthmuller, *Phys. Rev. B* **54**, 11169 (1996).

²⁶J. P. Perdew and Alex Zunger, *Phys. Rev. B* **23**, 5048 (1981).

²⁷J. P. Perdew, K. Burke, and M. Ernzerhof, *Phys. Rev. Lett.* **77**, 3865 (1996).

²⁸P. E. Blöchl, *Phys. Rev. B* **50**, 17953 (1994).

²⁹G. Kresse and D. Joubert, *Phys. Rev. B* **59**, 1758 (1999).

³⁰P. C. Newman, *J. Phys. Chem. Solids* **23**, 19 (1962).

³¹E. Finkman, J. Tauc, R. Kershaw, and A. Wold, *Phys. Rev. B* **11**, 3785 (1975).

³²N. Teraguchi, M. Konagai, F. Kato, and K. Takahashi, *J. Cryst. Growth* **115**, 798 (1991).

³³T. Nakayama and M. Ishikawa, *J. Phys. Soc. Jpn.* **66**, 3887 (1997).

- ³⁴M. Peressi and A. Baldereschi, *J. Appl. Phys.* **83**, 3092 (1998).
- ³⁵J. Heyd, G. E. Scuseria, and M. Ernzerhof, *J. Chem. Phys.* **118**, 8207 (2003).
- ³⁶J. Heyd and G. E. Scuseria, *J. Chem. Phys.* **121**, 1187 (2004).
- ³⁷J. Heyd, G. E. Scuseria, and M. Ernzerhof, *J. Chem. Phys.* **124**, 219906 (2006).
- ³⁸G. Henkelman, G. Johansson, and H. Jonsson, in *Progress in Theoretical Chemistry and Physics* (Kluwer Academic Publishers, Dordrecht, 2000), p. 269.
- ³⁹G. Henkelman, B. P. Uberuaga, and H. Jonsson, *J. Chem. Phys.* **113**, 9901 (2000).
- ⁴⁰The implementations of the climbing image nudged elastic band and the dimer method for VASP were obtained from <http://theory.cm.utexas.edu/henkelman>.
- ⁴¹G.-Y. Huang, C.-Y. Wang, and J.-T. Wang, *Solid State Commun.* **149**, 199 (2009).
- ⁴²G. Y. Huang, C. Y. Wang, and J. T. Wang, *J. Phys.: Condens. Matter* **21**, 195403 (2009).
- ⁴³A. Janotti and Chris G. Van de Walle, *Phys. Rev. B* **76**, 165202 (2007).
- ⁴⁴S. Lany and A. Zunger, *Phys. Rev. B* **78**, 235104 (2008).
- ⁴⁵C. G. Van de Walle, *J. Phys.: Condens. Matter* **20**, 064230 (2008).
- ⁴⁶R. M. Nieminen, *Modelling Simul. Mater. Sci. Eng.* **17**, 084001 (2009).
- ⁴⁷A. Alkauskas, P. Deák, J. Neugebauer, A. Pasquarello, and C. G. Van de Walle, *Phys. Status Solidi B* **248**, 17 (2011).
- ⁴⁸S. Lany and A. Zunger, *Modell. Simul. Mater. Sci. Eng.* **17**, 084002 (2009).
- ⁴⁹C. Freysoldt, J. Neugebauer, and C. G. Van de Walle, *Phys. Rev. Lett.* **102**, 016402 (2009).
- ⁵⁰C. Freysoldt, J. Neugebauer, and C. G. Van de Walle, *Phys. Status Solidi B* **248**, 1067 (2011).
- ⁵¹A. Alkauskas, P. Broqvist, F. Devynck, and A. Pasquarello, *Phys. Rev. Lett.* **101**, 106802 (2008).
- ⁵²A. Alkauskas, P. Broqvist, and A. Pasquarello, *Phys. Status Solidi B* **248**, 775 (2011).
- ⁵³A. Alkauskas and A. Pasquarello, *Phys. Rev. B* **84**, 125206 (2011).
- ⁵⁴G. Y. Huang, C. Y. Wang, and J. T. Wang, *Commun. Comput. Phys.* **183**, 1749 (2012).
- ⁵⁵H.-P. Komsa and A. Pasquarello, *Phys. Rev. B* **84**, 075207 (2011).
- ⁵⁶R. Ramprasad, H. Zhu, P. Rinke, and M. Scheffler, *Phys. Rev. Lett.* **108**, 066404 (2012).
- ⁵⁷F. Zheng, J. Shen, Y. Liu, W. Kim, M. Chu, M. Ider, X. Bao, and T. Anderson, *Calphad* **32**, 432 (2008).
- ⁵⁸M. Persin, B. Celustka, S. Popovic, and A. Persin, *Thin Solid Films* **37**, L61 (1976).
- ⁵⁹D. Lubbers and V. Leute, *J. Solid State Chem.* **43**, 339 (1982).
- ⁶⁰J. C. Mikkelsen, Jr., *J. Solid State Chem.* **40**, 312 (1981).
- ⁶¹F. Oba, M. Choi, A. Togo, and I. Tanaka, *Sci. Technol. Adv. Mater.* **12**, 034302 (2011).
- ⁶²F. Oba, A. Togo, I. Tanaka, J. Paier, and G. Kresse, *Phys. Rev. B* **77**, 245202 (2008).
- ⁶³G. Y. Huang and B. D. Wirth, *J. Phys.: Condens. Matter* **24**, 415404 (2012).
- ⁶⁴C. Rocha Leao and V. Lordi, *Phys. Rev. B* **84**, 165206 (2011).
- ⁶⁵T. Umeda, N. T. Son, J. Isoya, E. Janzen, T. Ohshima, N. Morishita, H. Itoh, A. Gali, and M. Bockstedte, *Phys. Rev. Lett.* **96**, 145501 (2006).
- ⁶⁶Y. Gai, J. Li, B. Yao, and J.-B. Xia, *J. Appl. Phys.* **105**, 113704 (2009).
- ⁶⁷P. Li, S. Deng, L. Zhang, G. H. Liu, and J. Yu, *Chem. Phys. Lett.* **531**, 75 (2012).
- ⁶⁸L. S. dos Santos, W. G. Schmidt, and E. Rauls, *Phys. Rev. B* **84**, 115201 (2011).